VTT Technical Research Centre of Finland

Superconducting insulators and localization of Cooper pairs

Arutyunov, Konstantin Yu; Lehtinen, Janne S.; Radkevich, Alexey; Semenov, Andrew G.; Zaikin, Andrei D.

Published in:
Communications Physics

DOI:
10.1038/s42005-021-00648-7

Published: 24/06/2021

Document Version
Publisher's final version

communications
physics

ARTICLE

https://doi.org/10.1038/s42005-021-00648-7 OPEN

Superconducting insulators and localization of Cooper pairs

Konstantin Yu. Arutyunov[1,2], Janne S. Lehtinen[3], Alexey Radkevich[4], Andrew G. Semenov[1,4] & Andrei D. Zaikin[4,5]✉

Rapid miniaturization of electronic devices and circuits demands profound understanding of fluctuation phenomena at the nanoscale. Superconducting nanowires – serving as important building blocks for such devices – may seriously suffer from fluctuations which tend to destroy long-range order and suppress superconductivity. In particular, quantum phase slips (QPS) proliferating at low temperatures may turn a quasi-one-dimensional superconductor into a resistor or an insulator. Here, we introduce a physical concept of QPS-controlled localization of Cooper pairs that may occur even in uniform nanowires without any dielectric barriers being a fundamental manifestation of the flux-charge duality in superconductors. We demonstrate – both experimentally and theoretically – that deep in the "insulating" state such nanowires actually exhibit non-trivial superposition of superconductivity and weak Coulomb blockade of Cooper pairs generated by quantum tunneling of magnetic fluxons across the wire.

[1] National Research University Higher School of Economics, Moscow, Russia. [2] P.L. Kapitza Institute for Physical Problems RAS, Moscow, Russia. [3] VTT Technical Research Centre of Finland Ltd., Centre for Metrology MIKES, Espoo, Finland. [4] I.E. Tamm Department of Theoretical Physics, P.N. Lebedev Physical Institute, Moscow, Russia. [5] Institute for Quantum Materials and Technologies, Karlsruhe Institute of Technology (KIT), Karlsruhe, Germany. ✉email: andrei.zaikin@kit.edu

Superconducting nanowires represent an important example of a system where low-temperature physics is dominated by both thermal and quantum fluctuations[1–5], thus making their properties entirely different from those of bulk superconductors well described by the standard Bardeen–Cooper–Schriffer (BCS) mean-field theory[6].

A large part of fluctuation phenomena in such nanowires are attributed to the so-called phase slips[1,2] which correspond to temporal local suppression of the superconducting order parameter $\Delta\exp(i\varphi)$ accompanied by the phase slippage process. At temperatures T close enough to the BCS critical temperature T_c such phase slips are induced by thermal fluctuations[7–9] whereas at lower temperatures $T \ll T_c$ quantum fluctuations of the order parameter take over and generate quantum phase slips (QPS)[10,11].

As the phase φ changes in time by 2π during a QPS event, each such event causes a voltage pulse $V = \dot{\varphi}/2e$ inside the wire. As a result, a current biased superconducting nanowire acquires a non-vanishing electric resistance down to lowest T[10,11]. This effect received its convincing experimental confirmation[12–18]. The same effect is also responsible for voltage fluctuations in superconducting nanowires[19,20]. Quantum phase slips also cause suppression of persistent currents in uniform superconducting nanorings[21,22].

A fundamentally important property of superconducting nanowires is the so-called flux-charge duality. This feature was extensively discussed for ultrasmall Josephson junctions[23–26] implying that under the duality transformation $2e \leftrightarrow \Phi_0$ quantum dynamics of Cooper pairs (with charge $2e$) should be identical to that of magnetic flux quanta $\Phi_0 = hc/2e$. All the same arguments remain applicable for shorter superconducting nanowires[27] which properties are dual to those of small Josephson junctions (Fig. 1). The duality considerations can further be extended to longer nanowires[5,22].

Manifestations of flux-charge duality in superconducting nanowires were observed in a variety of experiments thereby opening new horizons for applications of such structures in modern nanoelectronics, information technology, and metrology. These observations include, e.g., coherent tunneling of magnetic flux quanta through superconducting nanowires[28,29] and the so-called Bloch steps[30]. Operations of duality-based single-charge transistor[31,32] and charge quantum interference device[33] were demonstrated. Superconducting nanowires were also proposed to serve as central elements for QPS flux qubits[34] as well as for creating a QPS-based standard of electric current[35].

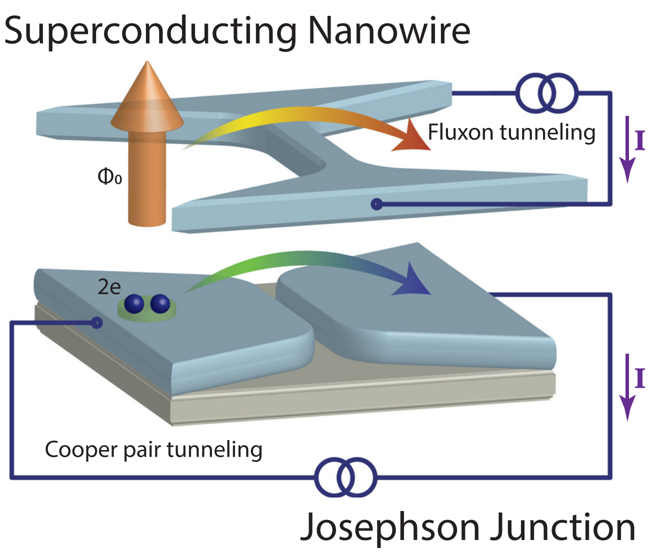

Fig. 1 Flux-charge duality. Quantum tunneling of a magnetic fluxon Φ_0 across a superconducting nanowire and a dual tunneling process of a Cooper pair with charge 2e across a Josephson junction between two superconductors.

Quantum fluctuations in superconducting nanowires are controlled by two different parameters

$$g_\xi = R_q/R_\xi \quad \text{and} \quad g_Z = R_q/Z. \tag{1}$$

Here $R_q = h/e^2 \simeq 25.8\,\text{k}\Omega$ is the quantum resistance unit, R_ξ is the normal state resistance of the wire segment of length equal to the superconducting coherence length ξ and $Z = \sqrt{\mathcal{L}/C}$ is the wire impedance determined by the kinetic wire inductance (times length) $\mathcal{L}$ and the geometric wire capacitance (per length) C.

The dimensionless conductance g_ξ accounts for the fluctuation correction to the BCS order parameter[9] $\Delta \to \Delta - \delta\Delta$ (with $\delta\Delta \sim \Delta/g_\xi$) and determines the QPS amplitude (per unit wire length)[11] $\gamma_{\rm qps} = b(g_\xi \Delta/\xi)\exp(-a g_\xi)$ (with $a \sim 1$ and $b \sim 1$). The dimensionless admittance g_Z, in turn, accounts for hydrodynamic (long wavelength) fluctuations of the superconducting phase intimately related to sound-like plasma modes[36] propagating along the wire with the velocity $v = 1/\sqrt{\mathcal{L}C}$. Different quantum phase slips interact by exchanging such plasmons and, hence, the parameter g_Z also controls the strength of inter-QPS interactions. By reducing the wire diameter $\sqrt{s} \propto g_Z$ one eventually arrives at the "superconductor-insulator" quantum phase transition[10] that occurs at $g_Z = 16$ and $T \to 0$.

In this work, we experimentally and theoretically investigate both global and local ground-state properties of superconducting nanowires in the "insulating" regime $g_Z < 16$. We demonstrate that quantum fluctuations of magnetic flux in long nanowires yield effective localization of Cooper pairs at a fundamental length scale L_c that essentially depends on both parameters (1). We also show that nominally uniform nanowires exhibit a non-trivial mixture of superconducting-like features at shorter length scales and resistive long-scale behavior which should actually tend to insulating at $T \to 0$. This state of matter can thus be named as a superconducting insulator.

Results

In order to accomplish our goal, we fabricated long and thin titanium nanowires having the form of narrow strips overlapping a relatively wide aluminum electrode through a tunnel barrier (aluminum oxide), as it is shown in Fig. 2. The normal state resistance of these wires R_N measured above the BCS critical temperature $T_c \approx 400$ mK was found in the range $R_N \sim 25$–70 kΩ. The length $L \simeq 20$ μm and thickness $d \simeq 35$ nm remain the same for all Ti samples, whereas their width w varies in the range 30–60 nm within which quantum phase slips usually proliferate in Ti nanowires[15,37]. The zero-temperature superconducting coherence length in our Ti samples is estimated to be $\xi \sim 140$–150 nm and, hence, the quasi-one-dimensional limit condition $d, w \ll \xi \ll L$ holds for all samples. With these parameters, one obtains the dimensionless admittance $g_Z \approx 1$–3, i.e., the desired condition $g_Z < 16$ is well satisfied in all our nanowires. The dimensions of the aluminum strip are large enough, enabling one to ignore fluctuation effects.

Nanowire resistance. The results of our measurements of a total resistance $R(T)$ for five different nanowires are displayed in Fig. 3a. With the values $g_Z \ll 16$, in the low-temperature limit all these samples should remain deep in the insulating regime. We observe, however, that two thicker samples with nominal widths $w \approx 62$ nm (sample Ti1) and $w \approx 46$ nm (sample Ti2), demonstrate a pronounced resistive behavior with $R(T) \approx R_N$ only at temperatures not far below the bulk titanium critical temperature $T_c \approx 400$ mK followed by a rather sharp resistance drop by ~2

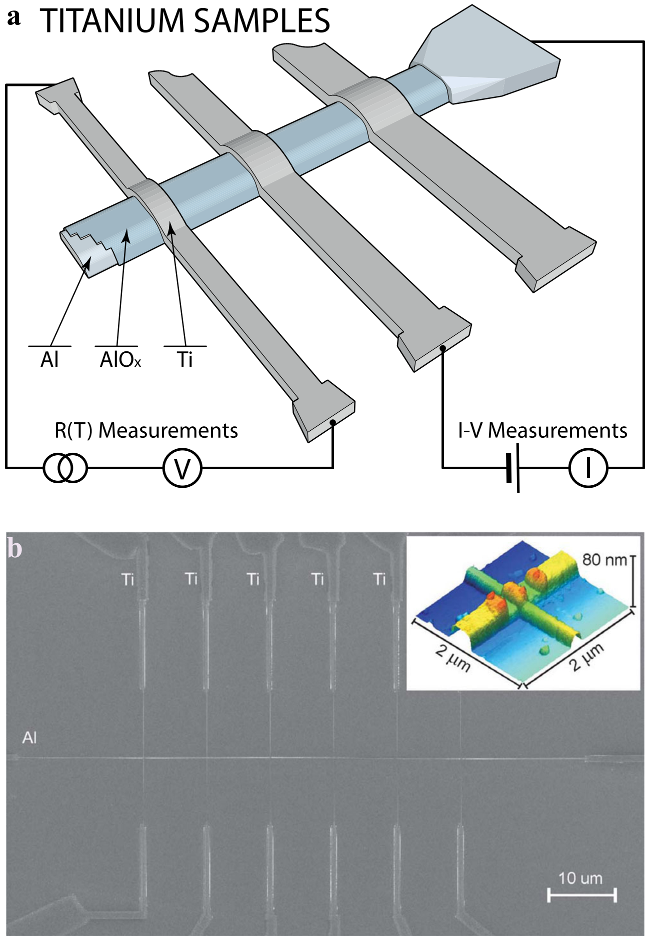

Fig. 2 Schematics of experiment and sample layout. a Long and thin titanium nanowires having the form of narrow strips overlap a relatively wide aluminum electrode through a tunnel barrier (aluminum oxide). The structure enables one to carry out both pseudo-four-terminal measurements of the total resistance for all nanowires and local measurements of the current-voltage characteristics for all Al-AlO_x-Ti tunnel junctions. **b** Scanning electron microscope image of our typical structure. Inset: Zoom of the junction region taken with atomic force microscope. Fake color corresponds to variation of the sample height from 0 (substrate, dark blue) to 80 nm (overlapping titanium, orange).

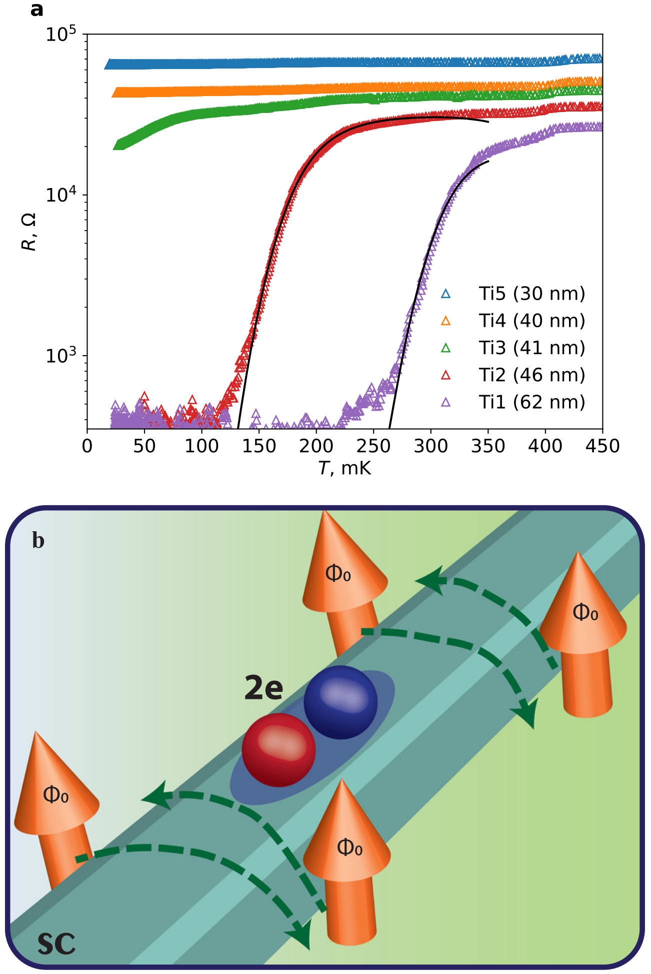

Fig. 3 Resistance data and localization of Cooper pairs. a Resistance versus temperature $R(T)$ measured for five Ti nanowires of length $L = 20$ µm, thickness $d \simeq 35$ nm, and nominal width values w indicated in brackets for each of the samples. Solid lines represent fits of the data for samples Ti1 and Ti2 to the theory[9] within its validity range. Resistance saturation observed in these two samples at low T is due to finite voltage sensitivity of about few nV corresponding to residual resistance ~100 Ω measured using ac bias current ~10 pA rms. Error bars are smaller than data points. **b** Localization of Cooper pairs (with charge 2e) generated by quantum tunneling of magnetic fluxons Φ_0 across the nanowire. This phenomenon explains the low-temperature behavior of $R(T)$ observed in samples Ti3, Ti4, and Ti5.

orders of magnitude at temperatures $T \sim 300$ mK (sample Ti1) and $T \lesssim 200$ mK (sample Ti2). The remaining samples Ti3, Ti4, and Ti5 with nominal widths just slightly below that for Ti2 (respectively, $w \approx 41$, 40, and 30 nm) show no sign of superconductivity down to the lowest T and only very weak dependence $R(T)$, in particular for the thinnest samples Ti4 and Ti5.

At temperatures not far below T_c the system behavior should be dominated by thermally activated phase slips which contribution to the wire resistance $R_{\rm taps}(T)$[9] indeed provides very accurate fits for the resistance of two of the above samples (see Fig. 3a) and allows to extract effective values $g_\xi \simeq 37.4$ and $g_\xi \simeq 9.0$, respectively, for samples Ti1 and Ti2 (see Supplementary Note 1 for more details). These values are smaller than the nominal ones, most likely indicating certain non-uniformity of our nanowires.

Localization of Cooper pairs. In order to understand drastic difference in the low-temperature behavior of our samples with various cross-sections it is necessary to account for the effect of quantum phase slips. The dual Hamiltonian for superconducting nanowires in the presence of QPS reads[5,22]

$$\hat{H} = \int_0^L dx \left[\frac{\hat{\Phi}^2}{2\mathcal{L}} + \frac{(\partial_x \hat{Q})^2}{2C} - \gamma_{\rm qps} \cos\left(\frac{\pi \hat{Q}}{e}\right) \right], \qquad (2)$$

where $\hat{\Phi}$ and $\hat{Q}$ are canonically conjugate flux and charge operators obeying the commutation relation $[\hat{\Phi}(x), \hat{Q}(x')] = -i\hbar\delta(x - x')$. Employing this Hamiltonian one can demonstrate[5,22] that in the "insulating" phase, i.e., for $g_Z < 16$, the wire ground-state properties are controlled by a non-perturbative correlation length $L_c \propto \gamma_{\rm qps}^{-\alpha}$ with $1/\alpha = 2 - g_Z/8$ or, equivalently,

$$L_c \sim \xi \exp\left(\frac{a g_\xi - \ln b}{2 - g_Z/8} \right). \qquad (3)$$

Physically the appearance of this QPS-induced fundamental length scale can be viewed as a result of spontaneous tunneling of magnetic flux quanta Φ_0 back and forth across the wire, as it is illustrated in Fig. 3b. These quantum fluctuations of magnetic flux wipe out phase coherence at distances $\sim L_c$ and yield effective localization of Cooper pairs at such length scales. Accordingly, samples with $L \lesssim L_c$ may still exhibit superconducting properties also in the presence of QPS, whereas in the limit $L \gg L_c$ the supercurrent gets disrupted by quantum fluctuations and such nanowires remain non-superconducting even at $T \to 0$.

This is exactly what the data in Fig. 3a demonstrate. Indeed, the value L_c (3) for the sample Ti1 with $g_\xi \approx 37$ obviously exceeds L by several orders of magnitude, and hence, this sample should remain superconducting at low enough T. In order to estimate the length scale (3) for sample Ti2 with $\xi \sim 140$ nm, $g_\xi \simeq 9.0$, and $g_Z \simeq 2.5$ it is desirable to explicitly determine the prefactors a and b. The data analysis for this sample yields a lower bound for the combination $ag_\xi - \ln b \gtrsim 7.5$, see Supplementary Note 2 for details. With this in mind, Eq. (3) allows to estimate $L_c \gtrsim 12$ μm, i.e., in this case, $L_c \sim L$ and the sample Ti2 should also remain superconducting at low T in accordance with our observations. By contrast, three thinner nanowires Ti3, Ti4, and Ti5 with lower effective values g_ξ and L_c significantly smaller than L exhibit a non-superconducting behavior down to lowest T.

In order to interpret this behavior let us recall that for $g_Z < 16$ quantum phase slips are no longer bound in pairs. According to the exact solution for the sine-Gordon model[38], in this case, an effective minigap in the spectrum $\tilde{\Delta} \propto \gamma_{\rm qps}^{\alpha}$ develops implying that at $T \to 0$ samples Ti3, Ti4, and Ti5 should behave as insulators. In line with these arguments, our resistance data in Fig. 3a demonstrate that the supercurrent in these samples is fully blocked by QPS down to the lowest available temperatures, and hence, their insulating behavior should indeed be expected at $T < \tilde{\Delta}$. The absence of any visible resistance upturn at low T most likely implies that the latter condition is not yet reached and/or the inequality $L \gg L_c$ is not satisfied well enough for these samples. In any event, here superconductivity is totally wiped out by quantum fluctuations in accordance with our theoretical arguments.

Note that the resistance data similar to those of Fig. 3a were also reported previously[12,13,39] for a large number of *MoGe* nanowires with shorter values of ξ and L. In some of these samples, the resistance upturn at lower T indicating the insulating behavior was observed. Reanalyzing the data[12,13,39] we conclude that they are also consistent with the above physical picture involving the correlation length L_c (3), i.e., the superconducting *MoGe* samples obey the condition $L \lesssim L_c$, whereas the non-superconducting ones typically have the length L exceeding L_c. Hence, retrospectively the observations[12,13,39] also receive a natural explanation which was not yet available at that time.

Local properties. Measurements of the total resistance $R(T)$ alone are not yet sufficient to obtain complete information about the quantum mechanical ground state of superconducting nanowires. In order to probe their local properties, we performed measurements of the I–V curves for tunnel junctions between Ti nanowires and bulk Al electrodes (with the BCS gap $\Delta_{\rm Al} \simeq 190$ μV), see Fig. 2. The corresponding results for all five samples are displayed in Fig. 4. In these samples, the differential conductance for Ti–Al tunnel junctions has a peak which position varies slightly from sample to sample. As the peak is expected to occur at $e|V| = \Delta + \Delta_{\rm Al}$, we immediately reconstruct the local gap value ranging between $\Delta \approx 50$ μeV and $\Delta \approx 37$ μeV depending on the sample. Hence, quantum fluctuations tend to reduce Δ in superconducting nanowires below its bulk value $\Delta_{\rm Ti} \simeq 60$ μeV and this effect appears more pronounced for thinner samples. On the other hand, a non-zero local superconducting gap Δ remains clearly observable in all our samples.

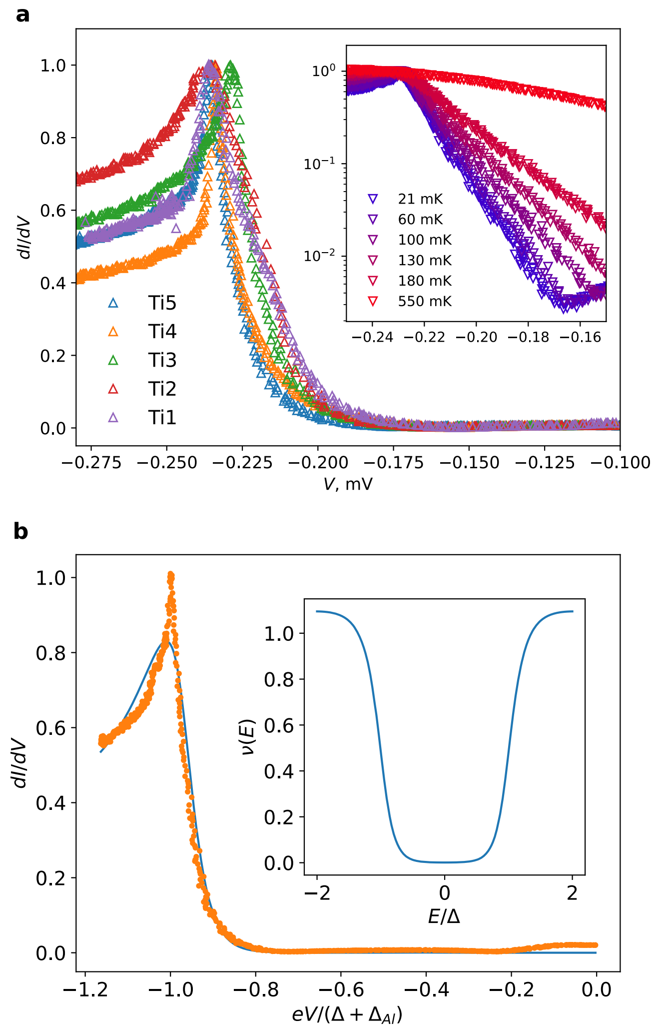

Fig. 4 Local differential conductance and electron density of states. **a** Differential conductance dI/dV as a function of voltage V measured in Ti−Al tunnel junctions at $T \simeq 21$ mK for five samples Ti1 to Ti5. A sharp peak is observed at $e|V| = \Delta + \Delta_{\rm Al}$. Inset: The same data for sample Ti3 at different temperatures. **b** Fit of the data for sample Ti3 at $T \simeq 21$ mK to the theory[40]. Inset: The density of states ν (in units of the normal density of states at the Fermi energy) as a function of energy E reconstructed for the same sample at the same T. Error bars are smaller than data points.

As compared to the standard BCS-like $I-V$ curve, systematic broadening of this peak in dI/dV with decreasing wire cross-section is observed. This broadening increases with T (cf. inset in Fig. 4a) and it can be explained[40,41] if we bear in mind that electrons exchange energies with an effective dissipative environment formed by Mooij–Schön plasmons propagating along the wire. As a result, in our Ti nanowires the singularity in the electron density of states (DOS) $\nu(E)$ at $|E| = \Delta$ and $T \to 0$ gets weaker with decreasing wire cross-section and becomes washed out by quantum fluctuations at $g_Z \lesssim 2$.

This is exactly what we observe in our experiment. By fitting the corresponding $I-V$ data for Ti−Al tunnel junctions to theoretical predictions[40] (see Supplementary Note 3) we reconstruct the energy-dependent DOS $\nu(E)$ for our Ti nanowires, as displayed in Fig. 4b. The best fit for sample Ti3 yields the value $g_Z \simeq 1.50$ just slightly below our theoretical estimate $g_Z \simeq 2.26$. In contrast to the standard BCS dependence $\nu_{\rm BCS}(E) = {\rm Re}|E|/\sqrt{E^2 - \Delta^2}$, here the gap singularities are totally smeared due to electron-plasmon interactions. Nevertheless the superconducting gap in DOS $\nu(E)$

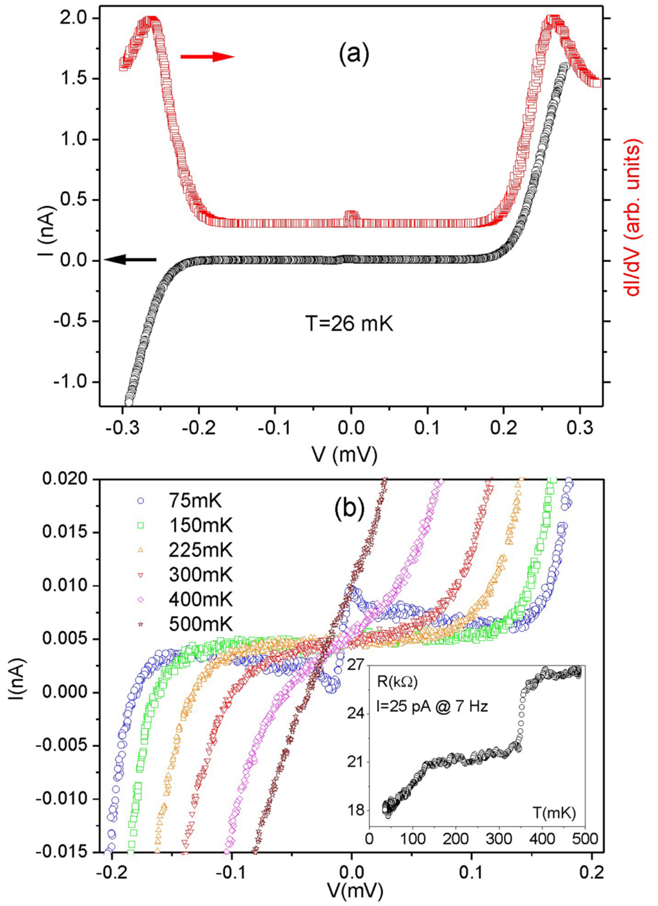

Fig. 5 Current–voltage characteristics and Josephson current. **a** Current-voltage characteristics for Ti-Al tunnel nanojunction corresponding to the Ti nanowire with $L = 20\,\mu$m, $d = 35$ nm, and $w = 38$ nm recorded at $T = 26$ mK. **b** Zoom of the current versus voltage dependencies taken at various temperatures. At $T \simeq 75$ mK one clearly observes the Josephson current which gradually disappears at higher T. Inset: The total resistance R measured for this nanowire as a function of temperature. Error bars are smaller than data points.

remains clearly visible. At non-zero T and subgap energies DOS decays exponentially with decreasing $|E|$ as $\nu(E) \propto \exp(-(\Delta - |E|)/T)$ (cf. inset in Fig. 4b) which is also due to the interaction between electrons and Mooij–Schön plasmons[40].

A pronounced superconducting gap in DOS is not the only feature indicating that locally superconducting properties remain preserved despite the effect of quantum fluctuations. In Fig. 5, we display the $I-V$ curves measured at different T for yet one more Ti nanowire with local DOS also showing a pronounced superconducting gap (Fig. 5a) and total resistance $R(T)$ behaving qualitatively similar to that of the samples Ti3, Ti4, and Ti5 (cf. inset in Fig. 5b). Zooming at the origin of these I–V curves we clearly observe the Josephson current ~5 pA at $T \simeq 75$ mK, see Fig. 5b. Quite naturally, due to strong fluctuation effects inside our Ti nanowire[42,43] this current value is orders of magnitude smaller than the nominal maximum Josephson current of few nA estimated from the standard Ambegaokar–Baratoff formula[6]. Fluctuation effects become even stronger with increasing temperature and totally wash out the Josephson current already at $T \gtrsim 150$ mK.

Note that the same Josephson current feature is detected in other Ti nanowires at low T and $V \to 0$, cf., e.g., Fig. 4a (inset) and Fig. 4b. These observations of dc Josephson effect in Ti–Al tunnel junctions further support our conclusion suggesting the presence of local superconductivity in all investigated Ti samples, including the most resistive ones.

Discussion

We arrive at the following physical picture describing ultrathin superconducting wires in the "insulating" regime $g_Z < 16$ at low enough temperatures. In this regime, QPS proliferate while TAPS effects can already be neglected. In thicker nanowires with $L_c \gtrsim L$ (samples Ti1 and Ti2) quantum phase slips alone cannot disrupt phase coherence across the wire. Such samples then behave to a large extent similarly to effectively zero-dimensional objects, such as, e.g., small-size Josephson junctions with the fluctuating phase[26] embedded in a low resistive external circuit. Depending on the experimental realization[22,42,43], these nanowires may either stay superconducting or become resistive, albeit typically with rather small $R \propto \gamma_{\rm qps}^2$. In contrast, thinner samples with $L_c \ll L$ remain highly resistive with $R \sim R_N$ even at $T \ll T_c$ and should turn insulating in the limit $T \to 0$. This behavior is due to QPS that suppresses long-range phase coherence in such nanowires.

Remarkably, the superconducting gap Δ in the energy spectrum of all our Ti nanowires, including highly resistive ones, is reduced but not destroyed by quantum fluctuations. In addition, this spectrum is also affected by the interaction between electrons and soft phase fluctuation modes (Mooij–Schön plasmons) which washes out the BCS gap singularity in DOS of ultrathin ($g_Z < 2$) nanowires and produces a weak subgap tail in $\nu(E)$ at non-zero T. We have demonstrated that the wire segments of length $\lesssim L_c$ retain their superconducting properties. On the other hand, longer nanowires composed of many such superconducting segments exhibit effective localization of Cooper pairs at lengths $\sim L_c$ and loose their ability to sustain any measurable supercurrent. These nanowires demonstrate a resistive behavior with $R(T) \sim R_N$ even at $T \ll T_c$ and should turn insulating in the limit of large L and $T \to 0$.

It is well-known that under certain conditions granular superconducting arrays and Josephson junction chains may also become resistive and even insulating[44–47]. In that regime, superconductivity is well preserved only inside grains while dissipativeless charge transfer across the system is prohibited due to Coulomb blockade of Cooper pair tunneling between such grains. Here, in contrast, we are dealing with nominally uniform nanowires which do not contain any grains and dielectric barriers at all. Nevertheless, such nanowires may exhibit both resistive and insulating behavior as long as their length L strongly exceeds the typical size of a "superconducting domain" $L_c \propto \gamma_{\rm qps}^{-\alpha}$. Similarly to normal metallic structures[1,48,49], this non-trivial feature can be interpreted as weak Coulomb blockade of Cooper pairs that—as it is illustrated by our results—may occur even in the absence of tunnel barriers.

In summary, we have demonstrated—both experimentally and theoretically—that long and uniform superconducting nanowires in the so-called "insulating" regime actually exhibit a more complicated behavior characterized by superposition of local superconductivity and effective global localization of Cooper pairs. This fundamental property of superconducting nanowires needs to be accounted for while designing various nanodevices with novel functionalities.

Methods

E-beam lift-off process, vacuum deposition of metals and in situ oxidation were used to fabricate tunnel junctions between aluminum electrodes and titanium nanostripes. Each structure enables one to carry out both pseudo-four-terminal measurements of the total resistance $R(T)$ for all Ti nanowires and local measurements of the $I-V$ curve for all Al−Ti tunnel junctions (Fig. 2). Differential conductances dI/dV were obtained by modulation technique using lock-in amplification. All experiments were made inside ^{3}He^{4}He dilution refrigerator with carefully filtered[50] input/output lines connecting sample to laboratory digital electronics through battery-powered analog pre-amplifiers (see Supplementary Note 4 for details).

Data availability

The data that support the findings of this study are available from K.Yu.A. (karutyunov@hse.ru) upon reasonable request.

Received: 18 December 2020; Accepted: 10 May 2021;
Published online: 24 June 2021

References

1. Zaikin, A. D. & Golubev, D. S. *Dissipative Quantum Mechanics of Nanostructures: Electron Transport, Fluctuations and Interactions* (Jenny Stanford Publishing, 2019).
2. Arutyunov, K. Y., Golubev, D. S. & Zaikin, A. D. Superconductivity in one dimension. *Phys. Rep.* **464**, 1 (2008).
3. Larkin, A. I. & Varlamov, A. A. *Theory of Fluctuations in Superconductors* (Clarendon Press, 2005).
4. Bezryadin, A. *Superconductivity in Nanowires* (Wiley-VCH, 2013).
5. Semenov, A. G. & Zaikin, A. D. Superconducting quantum fluctuations in one dimension. *Phys. Usp.* https://doi.org/10.3367/UFNe.2021.04.038962 (2021).
6. Tinkham, M. *Introduction to Superconductivity* (McGraw-Hill, 1996).
7. Little, W. A. Decay of persistent currents in small superconductors. *Phys. Rev.* **156**, 396–402 (1967).
8. McCumber, D. E. & Halperin, B. I. Time scale of intrinsic resistive fluctuations in thin superconducting wires. *Phys. Rev. B* **1**, 1054–1070 (1970).
9. Golubev, D. S. & Zaikin, A. D. Thermally activated phase slips in superconducting nanowires. *Phys. Rev. B* **78**, 144502 (2008).
10. Zaikin, A. D. et al. Quantum phase slips and transport in ultrathin superconducting wires. *Phys. Rev. Lett.* **78**, 1552 (1997).
11. Golubev, D. S. & Zaikin, A. D. Quantum tunneling of the order parameter in superconducting nanowires. *Phys. Rev. B* **64**, 014504 (2001).
12. Bezryadin, A., Lau, C. N. & Tinkham, M. Quantum suppression of superconductivity in ultrathin nanowires. *Nature* **404**, 971–973 (2000).
13. Lau, C. N. et al. Quantum phase slips in superconducting nanowires. *Phys. Rev. Lett.* **87**, 217003 (2001).
14. Zgirski, M. et al. Quantum fluctuations in ultranarrow superconducting aluminum nanowires. *Phys. Rev. B* **77**, 054508 (2008).
15. Lehtinen, J. S. et al. Evidence of quantum phase slip effect in titanium nanowires. *Phys. Rev. B* **85**, 094508 (2012).
16. Lehtinen, J. S. & Arutyunov, K. Y. The quantum phase slip phenomenon in superconducting nanowires with a low-Ohmic environment. *Supercond. Sci. Tech.* **25**, 124007 (2012).
17. Baumans, X. D. A. et al. Thermal and quantum depletion of superconductivity in narrow junctions created by controlled electromigration. *Nat. Commun.* **7**, 10560 (2016).
18. Arutyunov, K. Y. et al. Superconductivity in highly disordered NbN nanowires. *Nanotechnology* **27**, 47LT021 (2016).
19. Semenov, A. G. & Zaikin, A. D. Quantum phase slip noise. *Phys. Rev. B* **94**, 014512 (2016).
20. Semenov, A. G. & Zaikin, A. D. Full counting statistics of quantum phase slips. *Phys. Rev. B* **99**, 094516 (2019).
21. Arutyunov, K. Y. et al. Quantum phase slip phenomenon in ultra-narrow superconducting nanorings. *Sci. Rep.* **2**, 293–297 (2012).
22. Semenov, A. G. & Zaikin, A. D. Persistent currents in quantum phase slip rings. *Phys. Rev. B* **88**, 054505 (2013).
23. Zaikin, A. D. & Panyukov, S. V. Dynamics of a quantum dissipative system: duality between coordinate and quasimomentum spaces. *Phys. Lett. A* **120**, 306–311 (1987).
24. Averin, D. V. & Odintsov, A. A. Macroscopic quantum tunneling of the electric charge in small tunnel junctions. *Phys. Lett. A* **140**, 251–257 (1989).
25. Zaikin, A. D. Quantum dynamics of the charge in Josephson tunnel junctions. *J. Low Temp. Phys.* **80**, 223–235 (1990).
26. Schön, G. & Zaikin, A. D. Quantum coherent effects, phase transitions and the dissipative dynamics of ultra small tunnel junctions. *Phys. Rep.* **198**, 237–412 (1990).
27. Mooij, J. E. & Nazarov, Yu. V. Superconducting nanowires as quantum phase-slip junctions. *Nat. Phys.* **2**, 169–172 (2006).
28. Astafiev, O. V. et al. Coherent quantum phase slip. *Nature* **484**, 355–358 (2012).
29. Peltonen, J. T. et al. Coherent flux tunneling through NbN nanowires. *Phys. Rev. B* **88**, 220506(R) (2013).
30. Lehtinen, J. S., Zakharov, K. & Arutyunov, K. Y. Coulomb blockade and Bloch oscillations in superconducting Ti nanowires. *Phys. Rev. Lett.* **109**, 187001 (2012).
31. Hongisto, T. T. & Zorin, A. B. Single-charge transistor based on the charge-phase duality of a superconducting nanowire. *Phys. Rev. Lett.* **108**, 097001 (2012).
32. K, A., Yu. & Lehtinen, J. S. Junctionless Cooper pairt ransistor. *Physica C* **533**, 158–160 (2017).
33. De Graaf, S. E. et al. Charge quantum interference device. *Nat. Phys.* **14**, 590–595 (2018).
34. Mooij, J. E. & Harmans, C. J. P. M. Phase-slip flux qubits. *New. J. Phys.* **7**, 219 (2005).
35. Wang, Z., Lehtinen, J. S. & Arutyunov, K. Y. Towards quantum phase slip based standard of electric current. *Appl. Phys. Lett* **114**, 242601 (2019).
36. Mooij, J. E. & Schön, G. Propagating plasma mode in thin superconducting filaments. *Phys. Rev. Lett.* **55**, 114–117 (1985).
37. K, A., Yu. & Lehtinen, J. S. Quantum fluctuations of a superconductor order parameter. *Nanoscale Res. Lett.* **11**, 364 (2016).
38. Gogolin, A. O., Nersesyan, A. A. & Tsvelik, A. M. *Bosonization and Strongly Correlated Systems* (Cambridge University Press, 1998).
39. Bollinger, A. T. et al. Determination of the superconductor-insulator phase diagram for one-dimensional wires. *Phys. Rev. Lett.* **101**, 227003 (2008).
40. Radkevich, A., Semenov, A. G. & Zaikin, A. D. Quantum phase fluctuations and density of states in superconducting nanowires. *Phys. Rev. B* **96**, 085435 (2017).
41. Arutyunov, K. Y. et al. Smearing of electron density of states in quasi-one-dimensional superconducting channels due to quantum phase fluctuations. *J. Magn. Magn. Mat.* **459**, 356–358 (2018).
42. Radkevich, A., Semenov, A. G. & Zaikin, A. D. Quantum fluctuations and phase coherence in superconducting nanowires. *Phys. Rev. B* **100**, 014520 (2019).
43. Radkevich, A., Semenov, A. G. & Zaikin, A. D. Topology-controlled phase coherence and quantum fluctuations in superconducting nanowires. *J. Supercond. Nov. Magn.* **33**, 2335–2339 (2020).
44. Panyukov, S. V. & Zaikin, A. D. Quantum coherence and phase transitions in granular superconductors with dissipation. I. Ordered arrays. *J. Low Temp. Phys.* **75**, 361–388 (1989).
45. Fazio, R. & Schön, G. Charge and vortex dynamics in arrays of tunnel junctions. *Phys. Rev. B* **43**, 5307–5320 (1991).
46. Bobbert, P. et al. Phase transitions in dissipative Josephson chains: Monte Carlo results and response functions. *Phys. Rev. B* **45**, 2294–2304 (1992).
47. Fazio, R. & van der Zant, H. Quantum phase transitions and vortex dynamics in superconducting networks. *Phys. Rep.* **355**, 235–334 (2001).
48. Nazarov, Y. V. Coulomb blockade without tunnel barriers. *Phys. Rev. Lett.* **82**, 1245–1248 (1999).
49. Golubev, D. S. & Zaikin, A. D. Coulomb interaction and quantum transport through a coherent scatterer. *Phys. Rev. Lett.* **86**, 4887–4890 (2001).
50. Zavyalov, V. V. et al. Examination of cryogenic filters for a miltistage RF filtering system required for ultralow temperature experiments. *J. Phys.: Conf. Series* **969**, 012086 (2018).

Acknowledgements

A.R. acknowledges financial support from RFBR grant No. 19-32-90229. Experimental activity of K.Yu.A. has been supported by the “Mirror Lab” project of HSE University.

Author contributions

K.Yu.A. conceived the project, built the experimental set-up, performed measurements, and contributed to text writing. J.S.L. fabricated nanostructures, analyzed the structures with SEM and AFM, and performed measurements. A.R. contributed to the theory and performed fitting of experimental results to theory. A.G.S. contributed to theory and produced figures. A.D.Z. suggested the interpretation, contributed to theory, headed the theory team, and wrote the manuscript. All authors analyzed the data, discussed the results, and their interpretation.

Funding

Open Access funding enabled and organized by Projekt DEAL.

Competing interests

The authors declare no competing interests.

Additional information

Supplementary information The online version contains supplementary material available at https://doi.org/10.1038/s42005-021-00648-7.

Correspondence and requests for materials should be addressed to A.D.Z.

Peer review information *Communications Physics* thanks the anonymous reviewers for their contribution to the peer review of this work.